Experimental Analysis of Hole characteristics in Laser Micro-Drilling of Nitinol

P.P.S.Keerthi[1,2*], M.Sreenivasa Rao[3]

1. Research Scholar, Department of Mechanical Engineering, JNTU, Hyderabad, Telangana, India
2. Assistant Professor, Department of Mechanical Engineering, GVP College of Engineering(A), Visakhapatnam, Andhra Pradesh, India
3. Professor, Department of Mechanical Engineering, JNTU, Hyderabad, Telangana, India

Abstract: Nitinol is a nickel-titanium-based super alloy having unique properties like pseudo elasticity and shape memory. Applications of Nitinol range from medical devices, vibration damping, and temperature control to consumer goods. The high hardness of Nitinol makes it difficult to machine by conventional methods. Laser micromachining, a thermal-based non-conventional process, proved to be a promising technique to drill micro-holes with good dimensional accuracy. This paper investigates the hole characteristics like heat affected zone and circularity during laser micro-drilling of Nitinol for different values of sheet thickness, beam spot radius and feed rate. The effect of the input parameters on the hole quality has been discussed. Regression Analysis has been carried out to understand the influence of the parameters on the Heat affected zone and the circularity of the drilled holes.

Key Words: Nitinol, Laser micro-drilling, Circularity, Heat Affected Zone(HAZ), Regression Analysis

1. Introduction:

Advances in automotive, aerospace and medical industries call for the use of advanced materials like titanium, and nickel super-alloys. Nitinol is one such alloy of Nickel and Titanium, known for its properties like super-elasticity shape memory and high damping capacity[1].The uniqueness of Nitinol lies in the extent of modification that can be achieved by heat treatment, mechanical working and changes in composition[2]. Nitinol has high super elasticity, biocompatibility, kink and fatigue resistance, which makes it an excellent choice for medical devices. Nitinol is used to manufacture guidewires, catheter tubes, filters, stone retrieval baskets, needles, dental files, stents, arch wires and other surgical instruments[3]. Traditional machining methods for superalloys like Nitinol is very difficult due to their inherent mechanical and thermal properties [4]. The high hardness of the materials can result in high cutting forces due to the interaction between the tool and the workpiece[5]. High thermal stresses and heat-affected zones arise due to thermal properties like poor heat dissipation, conductivity etc. Also, the requirement for precise and intricate features like the fabrication of cardiac stents, cooling nozzles of turbine blades etc., need advanced machining processes. Laser micro drilling is one such non-contact machining process, which can produce precise holes of range micro and nanometres with minimal heat affected zone and adequate dimensional accuracy. Almost any known material can be machined by laser micro drilling[6]. Laser micromachining utilizes a focused laser beam directed on the workpiece surface to remove material by laser ablation. The excellent beam

quality of the lasers results in material processing and high precision for micro-manufacturing. Other advantages of the laser micromachining include high efficiency, compact installation size, easy integration and scalability[7].

Laser drilling is a complex phenomenon involving localized melting and vaporization. The application of laser micro drilling can be seen in aerospace, automotive, biomedical, micro-via hole drilling etc[8-9]. Laser drilling may be performed in different ways like trepanning and laser percussion drilling in both continuous and pulsed modes depending upon the diameter of the hole, and sheet thickness[10-11]. In percussion drilling, the material is irradiated by a focused beam at a single spot while in trepanning, material removal occurs in a circular pattern. Continuous laser beam drilling results in a higher heat-affected zone and problems due to the formation of the recast layer. Trepanning results in dimensionally precise holes with low heat-affected zones and in less time[8] and minimum hole diameter can be achieved in percussion drilling as compared to trepanning and helical drilling [12]. Helical drilling removes material through a helical path, dividing the length of the hole into several single passes[13-14].

Laser micromachining is a thermal energy-based process, that results in defects like Heat affected zone, due to the accumulation of heat around the irradiated zone, delamination of layers in composites, recast layer formation etc. The process is affected by several process parameters like lamp current, pulse repetition frequency(PRF), laser power, the wavelength of the laser, optical and thermal properties of the material etc.[13]. A thorough understanding of the influence of these parameters on the hole quality is important to achieve the required level of accuracy. Research shows considerable work on finding the optimal process parameters to achieve good-quality holes without loss of surface integrity. Chengal Reddy et.al observed that flushing pressure of 30Pa, 1500Hz PRF, 2000W laser can achieve minimized heat-affected zone and surface roughness during laser micro-drilling of different kinds of steels[14]. Laser micro-drilling on stainless steel foil for different values of pulse width, pulse frequency, and laser power, showed a significant improvement in the hole quality at low levels of the parameters with reduced spatters and recast layers[15]. Reduction in kerf width and surface roughness is observed for higher values of frequency and cutting speed and for low values of power and gas pressure during laser micro-cutting of mild steel[16]. During the laser micro-drilling on steel: SS-316L, Inconel-718 and Ti6Al4V, it was observed that the ovality of the hole is reduced by increasing the number of pulses. Also, material properties like low absorptive power and low focusing efficiency tend to increase ovality. Lower thermal conductivity tends to reduce hole taper[12]. The material properties also influence the dimensional accuracy of the hole and the area of the heat-affected zone[17]. The study of the literature shows that there is a wide scope to further improve the dimensional accuracy of the drilled holes in difficult–to–machine materials.

In this work, laser micro drilling has been performed on a super-alloy, Nitinol with sheet thickness, laser spot diameter and feed rate as process parameters. The obtained geometrical features are studied by a confocal microscope. Regression Analysis has been conducted to predict the effect of feed rate, spot diameter and sheet thickness on the hole quality characteristics like circularity and heat-affected zone.

2. Experimental work

In the present work, Nitinol sheets of size 100*100 in three different thicknesses (0.2, 0.3 and 0.5 mm) are taken for carrying out the experiments. The Nitinol sheets are supplied by

Manhar Metal Corporation, Mumbai. The composition and properties of Nitinol are listed in Table 1&2:

Table 1 Composition of Nitinol

Ti	Ni	Co	Cu	Cr
44.03	55.96	<0.01	<0.005	<0.005

Table -2 Properties of Nitinol[2]

Transformation Temperature	-200-100^{0}C
Latent heat of Transformation	5.78cal/g
Melting point	1300^{0}C
Density	6.45g/cc
Thermal conductivity(Austenite)	0.18 W/cm * deg. C (10.4 BTU/ft * hr * deg. F)
Thermal conductivity(Martensite)	0.086 W/cm * deg. C (5.0 BTU/ft * hr * deg. F)
Coefficient of thermal expansion(Austenite)	11.0E-6/deg. C (6.11E-6/deg. F)
Coefficient of thermal expansion(Martensite)	6.6E-6/deg. C (3.67E-6/deg. F)
Specific heat	0.20 cal/g * deg. C (0.20 BTU/lb * deg. F)
Young's modulus(Austenite)	approx. 83 GPa (12E6 psi)
Young's modulus(Martensite)	approx. 28 to 41 GPa (4E6 to 6E6 psi)
Yield strength(Austenite)	195 to 690 MPa (28 to 100 ksi)
Yield strength(Martensite)	70 to 140 MPa (10 to 20 ksi)
Ultimate tensile strength(Fully annealed)	895 MPa (130 ksi)
Ultimate tensile Strength(Work hardened)	1900 MPa (275 ksi)
Poisson's Ratio	0.33
Elongation at failure(Fully annealed)	25 to 50%
Elongation at failure(work hardened)	5 to 10%

3. Experimental setup:

Present experiments are carried out using the Solid-state Nd: Yag Femto second Laser Micro Machining system with a water cooling system at Central Manufacturing Technology Institute, Banglore. The present setup uses nitrogen gas as an assist gas with a water cooling system. The laser drilling system consists of the delivery of a laser head, a worktable to position the workpiece and an optical system to achieve the focusing. The relative motion between the workpiece and the lasers is obtained by fixing the laser and movable worktable. A CNC drilling code is prepared with the required parameters to carry out the drilling of the holes in trepanning mode. The micromachining system is shown in Fig-1 and system specifications are given in Table 3.

Table-3. Specifications of the Micromachining system

Average power	2.5W
Laser wavelength	775 nm
Minimum feature size	1 µm
Pulse width	10ps-150fs

Resolution	1nm
Traverse X, Y & Z Axis	150 x 150 x 100 mm
Pulse repetition rate	1 Hz to 2 KHz
Lamp Current	21.1 Amp

Figure-1.a: Image of the femtosecond laser Micro Machining System

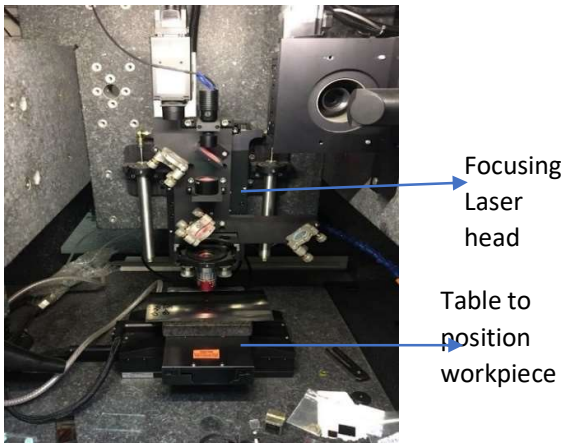

1. b Laser Micromachining Setup

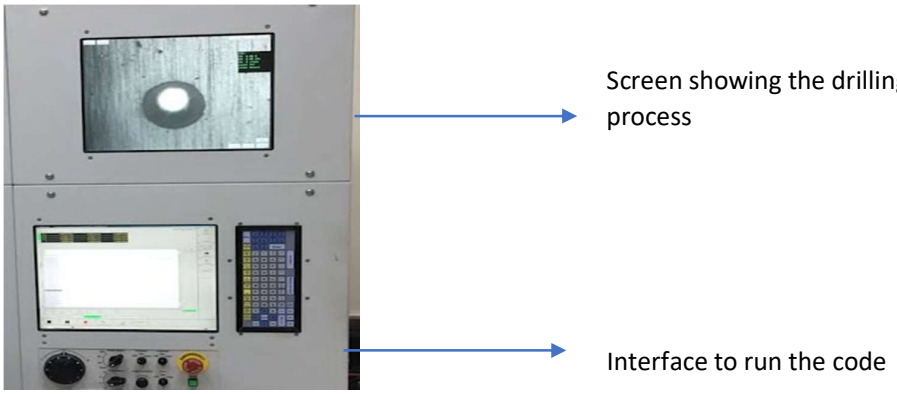

1. c. Screen showing the drilling process

4. Input parameters levels

Laser micro drilling is influenced by three important parameters considered in this work, feed rate, hole spot diameter and the thickness of the worksheet. These parameters have been identified based on their influence on the hole quality during laser micro-drilling.

The feed rate in Laser micromachining is the linear speed at which the laser beam interacts with the material removing the generation of the required features[18]. An increasing feed rate combined with low laser power reduces the time of interaction with the material, resulting in holes of lower diameter and decreased HAZ.The feed rate also affects the surface roughness, the value increasing with increasing feed rate[19-21]. Increased feed

rates also tend to decrease the depth of the laser-machined channels, thereby resulting in a low aspect ratio of the channels[22].

Sheet thickness is another parameter that influences the accuracy of hole formation in laser micro-drilling. Workpiece thickness alters the energy required for full-depth penetration cutting. The focal setting corresponding to the minimum kerf size changes with an increase in the workpiece thickness[23]. Also, as the sheet thickness increases, the depth of the drilled hole increases, thereby increasing the aspect ratio of drilled holes. High values of aspect ratio influence the power requirements, recast layer formation, penetration laser beam to produce the hole, taper formation of the holes etc[24].

The laser spot diameter is affected by the laser power and power density. A larger diameter affects a wider zone on the workpiece and also increases the energy absorbed[25]. The spot diameter of the Gaussian laser beam directly influences the specific material removal rate, the latter decreasing with an increase in the spot diameter[26].

The different levels of parameters used in the experimentation are shown in the table-4

Table 4: Parameter Levels

Parameter	Level-1	Level 2	Level-3
Sheet Thickness(mm)	0.2	0.3	0.5
Feed Rate(mm/s)	0.1	0.5	1
Spot Diameter(µs)	150	225	300

The drilled holes are measured using Olympus 3D measuring laser microscope LEXT OLS4000 designed for nanometre level imaging, 3D measurement and roughness measurement. Magnification ranges from 108x - 17,280x. The measurements are carried out at the entry and exit of the hole. Two diameters d1 and d2 are measured at 90^0 intervals for each hole at entry and exit. The average diameters at entry and exit are calculated as:

$$d_{entry} = \left(\frac{d_1+d_2}{2}\right) \quad (1)$$

$$d_{exit} = \left(\frac{d_3+d_4}{2}\right) \quad (2)$$

5. Hole quality Characteristics:

Two-hole characteristics are considered in the present work, hole circularity and heat-affected zone thickness. As the beam propagates through the material, the area around the irradiated zone undergoes microstructural changes and is termed as heat affected zone[27]. The maximum diameter for each hole is measured at 900 intervals as h1 and h2. The average HAZ thickness at the hole entry can be obtained as:

$$HAZ = \left(\frac{d_{exit}-d_{entry}}{2}\right) \quad (3)$$

The hole circularity is defined as the ratio of the minimum hole diameter to the maximum hole diameter.

$$C_{entry} = \left(\frac{\min(d_{entry},d_{exit})}{\max(d_{entry},d_{exit})}\right) \quad (4)$$

The two characteristics have been calculated for all the drilled holes and the values are obtained as follows:

Table 5: Obtained values of HAZ and Circularity

Ex. No	Diameter (um)	Thickness (mm)	feed rate (mm/s)	Average HAZ at Entry	circularity entry
1	150	0.2	0.1	52.8205	0.968861
2	150	0.3	0.5	63.4730	0.941726
3	150	0.5	1.0	93.1770	0.958405
4	225	0.2	0.5	55.2975	0.963133
5	225	0.3	1.0	51.5830	0.991944
6	225	0.5	0.1	86.0570	0.968097
7	300	0.2	1.0	94.6215	0.988553
8	300	0.3	0.1	63.6670	0.940982
9	300	0.5	0.5	33.2635	0.926601

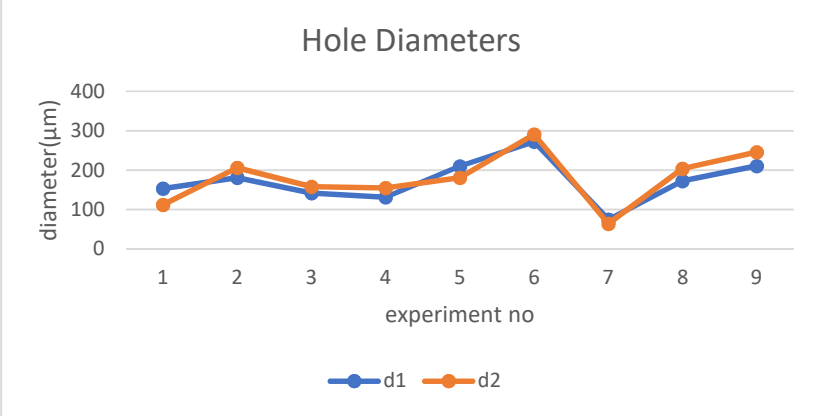

Fig-2: Diameters of hole

6. Regression model:

To identify the relationship between the independent and dependent variables, regression analysis can be used. the relationship is hypothesized, and estimates of the parameter values are used to develop an estimated regression equation. [28]. Several linear and nonlinear regression models are available to model the relation between the process variables and the performance characteristics [29]. A general-order linear regression is given by

$$y = \beta_{0+} \sum_{i-1}^{n} \beta_0 X_i + \sum_{i-1}^{n} \beta_{ii} X^2{}_{i+} \sum_{i-1}^{n} \sum_{j-n+1}^{n} \beta_{ij} X_i X_j$$

(5)

Where Y is the dependent or the response variable, X is the predictor variable. β_is are the regression coefficients [30]. The values of regression coefficients can be obtained by the method of least squares[10]. Minitab 17 develop the regression models for Heat affected zone and the circularity at the entry. In the present model, the effect of interactions through an order of 3 and terms through an order of 3 has been used. In the developed equations, the cubic terms have been eliminated as their effects on the response cannot be estimated. The developed models for heat affected zone and the hole circularity are given by:

$$HAZ = 59.3 + (148 * t) - (0.17 * d) - (46.7 * f) + (87 * t^2) + (0.00048 * d^2) + (26 * f^2) - (0.0726 * t * d) + (15 * t * f) + (0.5 * d * f) - (0.6 * t * d * f)$$

(6)

$$circularity = 2.88 + (5.2 * t) - (0.0263 * d) - (3.03 * f) - (12.8 * t^2) + (0.000066 * d^2) - (0.09 * f^2) + (3 * t * f) + (0.0222 * d * f) + (0.0421 * t^2 * d) - (1.7 * t^2 * f) - (0.000057 * t * d^2) - (0.0123 * t * d * f) + (0.97 * t * f^2) - (0.000042 * d^2 * f) + (0.0008 * d * f^2)$$

(7)

Where

t- thickness of sheet(mm),

d- spot diameter (µm)

f- feed rate in mm/s

The measurement of the diameters in the holes is shown in figure-3:

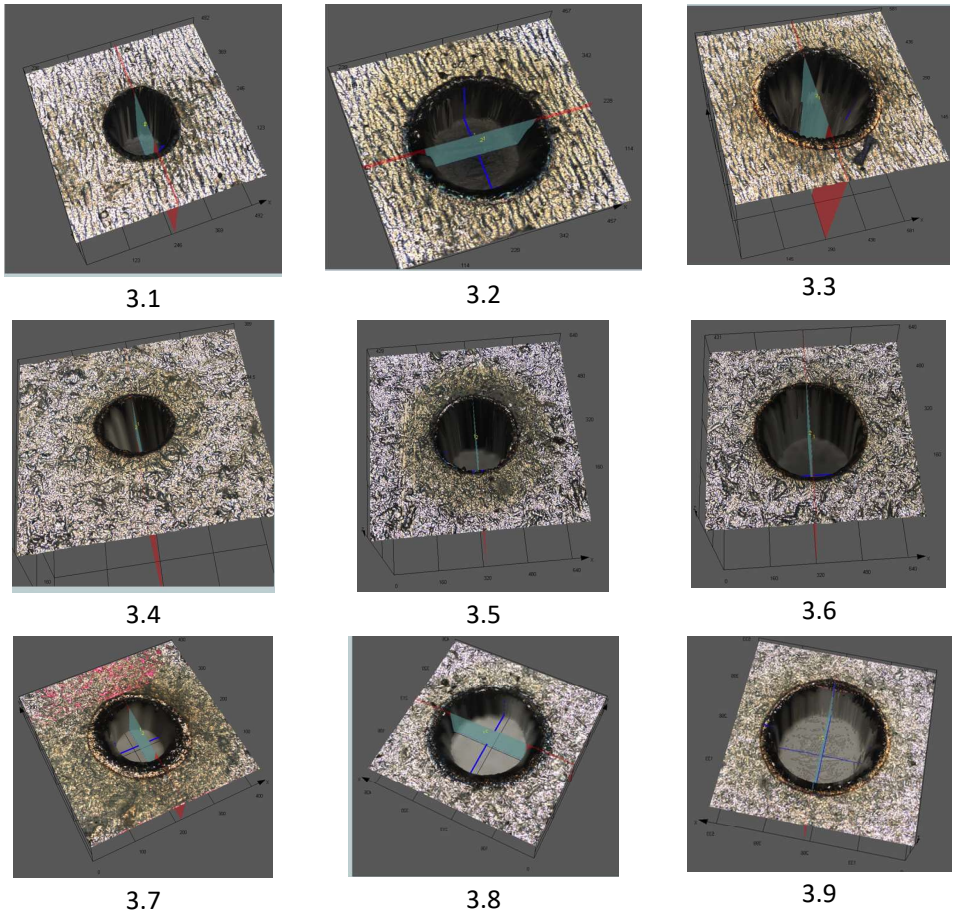

Figure 3: Measurement of hoe diameters in the order of experiment number

For the developed models of HAZ and hole circularity, the

S R-sq R-sq(adj) R-sq(pred)

Circularity	0.217102	46.52%	0.00%	0.00%
HAZ	11.8378	85.07%	61.19%	0.00%

The R2 also called the coefficient of determination is a measure of the scatter of the data points around the regression line. A higher value of R2 indicates of lower deviation between the experimental and the fitted values of the regression equation[31]. On the other hand, the S value represents the average distance of the data points from the regression line. A lower value of S is preferred as it shows that the observed values are close to the regression line[32].

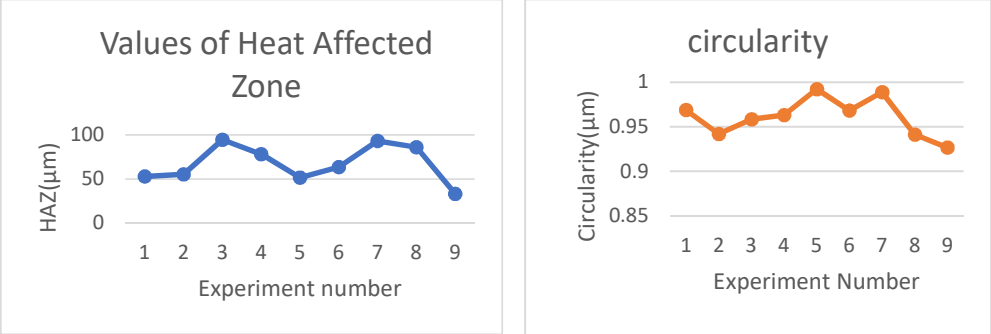

Figure 4: Values of Heat Affected Zone and Hole circularity at entry

7. Results and Discussions:

Signal-to-noise ratio analysis has been performed which is used to measure the robustness of the developed model and can help identify the factors settings that can reduce the effect of noise on the response variables. They predict how the response varies relative to the target value for different noise conditions. In this present work, it is desired to have a minimal value of HAZ and hole circularity is to be maximized. The optimal value for the hole circularity would be close to 1, as it indicates that hole diameters at entry and exit are the same. So, a signal-to-noise ratio of smaller is better is selected for HAZ while larger is better for the hole circularity. [29]

The table below shows the Response Table for Signal Noise Ratios which means for smaller is better for HAZ. From the table, it can be observed that spot diameter is more significant in determining HAZ values followed by feed rate and thickness.

Smaller is better

Level	Thickness	Diameter	Feed rate
1	-35.65	-37.22	-34.75
2	-35.67	-35.51	-35.04
3	-35.61	-34.18	-37.13
Delta	0.06	3.04	2.38
Rank	3	1	2

Response Table for Means

Level	T	D	F
1	63.21	73.80	57.56

2	61.82	61.65	58.99
3	65.35	54.91	73.81
Delta	3.53	18.89	16.25
Rank	3	1	2

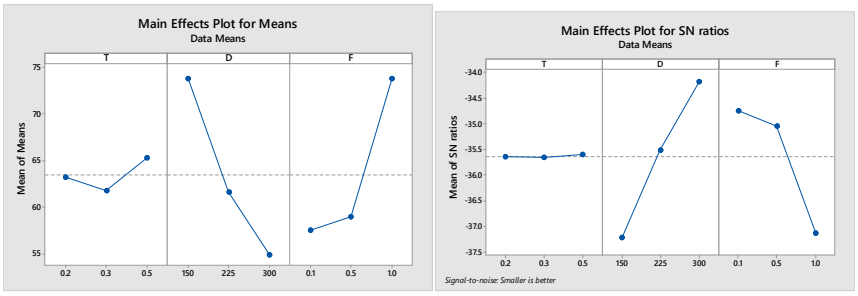

Figure 5: Plot of Main effects and SN ratios for HAZ

This table shows the signal-to-noise ratio for larger is better for Circularity at the hole entrance. It can be inferred that spot diameter is having more influence on the hole circularity followed by thickness and feed rate.
Response Table for Signal-to-Noise Ratios

Larger is better

Level	T	D	F
1	-2.038	-1.984	-2.031
2	-1.517	-3.917	-3.510
3	-3.780	-1.433	-1.793
Delta	2.263	2.484	1.717
Rank	2	1	3

Response Table for Means

Level	T	D	F
1	0.8071	0.8108	0.8031
2	0.8547	0.6918	0.7292
3	0.6948	0.8540	0.8242
Delta	0.1599	0.1622	0.0950
Rank	2	1	3

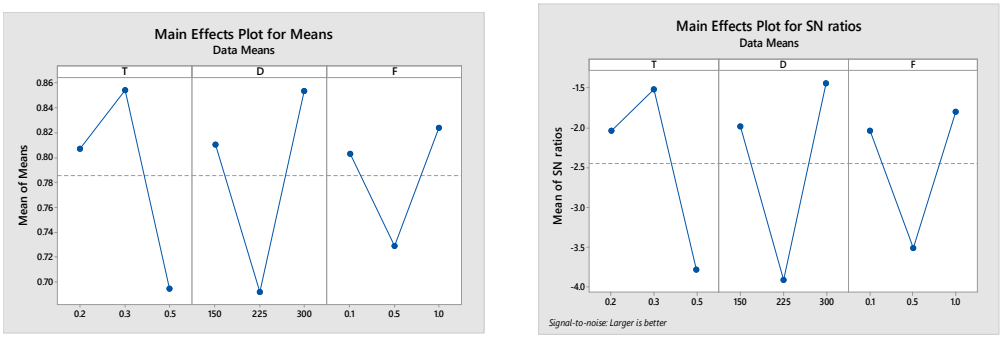

Figure 6: Plot of Main effects and SN ratios for Circularity

8. Conclusions:

The following conclusions were made from the present work:

1. Laser helical drilling of Nitinol Superalloy using a femtosecond laser has been performed with feed rate, spot radius and material thickness as process variables.
2. The regression analysis has been developed to understand the influence of these variables on HAZ and circularity.
3. From the Taguchi analysis of the developed model, it is observed that laser spot diameter has the maximum influence on the HAZ and the hole circularity.
4. From the developed regression equations, the minimal value of HAZ thickness of 32.25 µm is observed at 0.5mm thickness, 300µm spot diameter and a feed rate of 0.5mm/s.
5. The developed regression equation for hole circularity gives the best value of 0.969 at 0.3mm sheet thickness, 150Um dia and 0.1mm/s feed rate.

References:

[1] S. Alipour, F. Taromian, E. R. Ghomi, M. Zare, S. Singh, and S. Ramakrishna, "Nitinol: From historical milestones to functional properties and biomedical applications," *Proc. Inst. Mech. Eng. [H]*, p. 095441192211231, Sep. 2022, doi: 10.1177/09544119221123176.

[2] "Nitinol technical properties | Johnson Matthey." https://matthey.com/en/products-and-services/medical-components/resource-library/nitinol-technical-properties (accessed May 04, 2022).

[3] D. Kapoor, "Nitinol for Medical Applications: A Brief Introduction to the Properties and Processing of Nickel Titanium Shape Memory Alloys and their Use in Stents," *Johns. Matthey Technol. Rev.*, vol. 61, no. 1, pp. 66–76, Jan. 2017, doi: 10.1595/205651317X694524.

[4] K. E. Hazzan, M. Pacella, and T. L. See, "Laser Processing of Hard and Ultra-Hard Materials for Micro-Machining and Surface Engineering Applications," *Micromachines*, vol. 12, no. 8, p. 895, Jul. 2021, doi: 10.3390/mi12080895.

[5] M. Mehrpouya, A. M. Shahedin, S. Daood Salman Dawood, and A. Kamal Ariffin, "An investigation on the optimum machinability of NiTi based shape memory alloy," *Mater. Manuf. Process.*, vol. 32, no. 13, pp. 1497–1504, Oct. 2017, doi: 10.1080/10426914.2017.1279290.

[6] K. T. Voisey, "Laser Drilling of Metallic and Nonmetallic Materials and Quality Assessment," in *Comprehensive Materials Processing*, Elsevier, 2014, pp. 177–194. doi: 10.1016/B978-0-08-096532-1.00919-5.

[7] U. Klotzbach, A. F. Lasagni, M. Panzner, and V. Franke, "Laser Micromachining," in *Fabrication and Characterization in the Micro-Nano Range*, vol. 10, F. A. Lasagni and A. F. Lasagni, Eds. Berlin, Heidelberg: Springer Berlin Heidelberg, 2011, pp. 29–46. doi: 10.1007/978-3-642-17782-8_2.

[8] L. Li, "2 - The challenges ahead for laser macro, micro, and nano manufacturing," in *Advances in Laser Materials Processing*, J. Lawrence, J. Pou, D. K. Y. Low, and E. Toyserkani, Eds. Woodhead Publishing, 2010, pp. 20–39. doi: 10.1533/9781845699819.1.20.

[9] G. Chryssolouris and K. Salonitis, "Fundamentals of laser machining of composites," in *Machining Technology for Composite Materials*, Elsevier, 2012, pp. 266–287. doi: 10.1533/9780857095145.2.266.

[10] K. L. Dhaker and A. K. Pandey, "Particle Swarm Optimisation of Hole Quality Characteristics in Laser Trepan Drilling of Inconel 718," *Def. Sci. J.*, vol. 69, no. 1, pp. 37–45, Jan. 2019, doi: 10.14429/dsj.69.12879.

[11] A. K. Nath, "9.06 - Laser Drilling of Metallic and Nonmetallic Substrates," in *Comprehensive Materials Processing*, S. Hashmi, G. F. Batalha, C. J. Van Tyne,

and B. Yilbas, Eds. Oxford: Elsevier, 2014, pp. 115–175. doi: 10.1016/B978-0-08-096532-1.00904-3.

[12] G. Dongre, R. Gondil, A. Rajurkar, and J. Philip, "High Aspects Ratio Micro-drilling of Super-alloys Using Ultra Short Pulsed Laser," Dec. 2017.

[13] S. Mishra and V. Yadava, "Laser Beam MicroMachining (LBMM) – A review," *Opt. Lasers Eng.*, vol. 73, pp. 89–122, Oct. 2015, doi: 10.1016/j.optlaseng.2015.03.017.

[14] V. Chengal Reddy, T. Keerthi, T. Nishkala, and G. Maruthi Prasad Yadav, "Analysis and optimization of laser drilling process during machining of AISI 303 material using grey relational analysis approach," *SN Appl. Sci.*, vol. 3, no. 3, p. 335, Mar. 2021, doi: 10.1007/s42452-021-04337-6.

[15] G. Casalino, A. M. Losacco, A. Arnesano, F. Facchini, M. Pierangeli, and C. Bonserio, "Statistical Analysis and Modelling of an Yb: KGW Femtosecond Laser Micro-drilling Process," *Procedia CIRP*, vol. 62, pp. 275–280, 2017, doi: 10.1016/j.procir.2016.06.111.

[16] S. S. Patel, V. H. Patel, K. M. Patel, B. A. Patel, A. A. Patel, and S. C. Patel, "Experimental Analysis of Laser Cutting Machine," *Int. J. Eng. Res. Technol.*, vol. 10, no. 4, Apr. 2021, doi: 10.17577/IJERTV10IS040093.

[17] E. Kaselouris *et al.*, "Analysis of the Heat Affected Zone and Surface Roughness during Laser Micromachining of Metals," *Key Eng. Mater.*, vol. 827, pp. 122–127, Dec. 2019, doi: 10.4028/www.scientific.net/KEM.827.122.

[18] H. Lavvafi, "EFFECTS OF LASER MACHINING ON STRUCTURE AND FATIGUE OF 316LVM BIOMEDICAL WIRES," phd, CASE WESTERN RESERVE UNIVERSITY, CLEVELAND, Ohio, 2013.

[19] N. Rajaram, J. Sheikh-Ahmad, and S. H. Cheraghi, "CO2 laser cut quality of 4130 steel," *Int. J. Mach. Tools Manuf.*, vol. 43, no. 4, pp. 351–358, Mar. 2003, doi: 10.1016/S0890-6955(02)00270-5.

[20] K. A. Ghany and M. Newishy, "Cutting of 1.2mm thick austenitic stainless steel sheet using pulsed and CW Nd:YAG laser," *J. Mater. Process. Technol.*, vol. 168, no. 3, pp. 438–447, Oct. 2005, doi: 10.1016/j.jmatprotec.2005.02.251.

[21] M. Younes, H. Hof, and A. Khair, "Some quality in aspects of microdrilling using CO 2 pulsed laser," vol. 43, Sep. 2004.

[22] S. Bhandari, M. Murnal, J. Cao, and K. Ehmann, "Comparative Experimental Investigation of Micro-channel Fabrication in Ti Alloys by Laser Ablation and Laser-induced Plasma Micro-machining," *Procedia Manuf.*, vol. 34, pp. 418–423, 2019, doi: 10.1016/j.promfg.2019.06.186.

[23] C. Karatas, O. Keles, I. Uslan, and Y. Usta, "Laser cutting of steel sheets: Influence of workpiece thickness and beam waist position on kerf size and stria formation," *J. Mater. Process. Technol.*, vol. 172, no. 1, pp. 22–29, Feb. 2006, doi: 10.1016/j.jmatprotec.2005.08.017.

[24] V. Nasrollahi, P. Penchev, T. Jwad, S. Dimov, K. Kim, and C. Im, "Drilling of micron-scale high aspect ratio holes with ultra-short pulsed lasers: Critical effects of focusing lenses and fluence on the resulting holes' morphology," *Opt. Lasers Eng.*, vol. 110, pp. 315–322, Nov. 2018, doi: 10.1016/j.optlaseng.2018.04.024.

[25] K. Ding and L. Ye, "Physical and mechanical mechanisms of laser shock peening," in *Laser Shock Peening*, Elsevier, 2006, pp. 7–46. doi: 10.1533/9781845691097.7.

[26] M. Chaja, T. Kramer, and B. Neuenschwander, "Influence of laser spot size and shape on ablation efficiency using ultrashort pulse laser system," *Procedia CIRP*, vol. 74, pp. 300–304, Jan. 2018, doi: 10.1016/j.procir.2018.08.119.

[27] A. Jain, B. Singh, and Y. Shrivastava, "Analysis of heat affected zone (HAZ) during micro-drilling of a new hybrid composite," in *Proceedings of the Institution of Mechanical Engineers, Part C*, Sep. 2019. doi: 10.1177/0954406219877911.

[28] "https://www.britannica.com/science/statistics." https://www.britannica.com/science/statistics

[29] D. C. Montgomery, *Design and analysis of experiments*, Eighth edition. Hoboken, NJ: John Wiley & Sons, Inc, 2013.
[30] H. Guo and A. Mettas, "Design of Experiments and Data Analysis," in *2012 Annual RELIABILITY and MAINTAINABILITY Symposium*, 2012.
[31] "How To Interpret R-squared in Regression Analysis - Statistics By Jim." https://statisticsbyjim.com/regression/interpret-r-squared-regression/ (accessed Oct. 01, 2022).
[32] M. B. Editor, "Regression Analysis: How to Interpret S, the Standard Error of the Regression." https://blog.minitab.com/en/adventures-in-statistics-2/regression-analysis-how-to-interpret-s-the-standard-error-of-the-regression (accessed Oct. 01, 2022).